INTERNATIONAL SYMPOSIUM ON GLASS SCIENCE & TECHNOLOGY
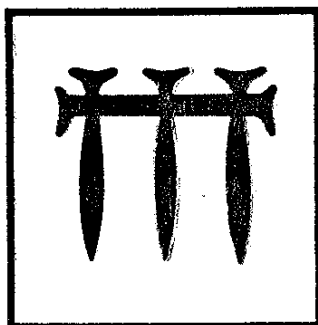
October 6-8, 1993
Athens, Greece

Organized by the
HELLENIKOS HYALOURGIKOS SYNDESMOS
(Greek Glass Federation)

Under the auspices of the
INTERNATIONAL COMMISSION ON GLASS

Proceedings of the
INTERNATIONAL SYMPOSIUM
ON GLASS SCIENCE AND TECHNOLOGY

Athens, 6-8 October 1993

Editors: G. D. Chryssikos and E. I. Kamitsos

PHYSICAL PROPERTIES AND SPECTROSCOPY OF RUBIDIUM AND CAESIUM BORATE GLASSES WITH EXCEPTIONALLY HIGH ALKALI CONTENT

S. FELLER, S. NIJHAWAN, M. ROYLE, J. MACKENZIE, J. TAYLOR, M. SHARMA
Physics Department, Coe College, Cedar Rapids, IA 52402, USA
E.I. KAMITSOS, G.D. CHRYSSIKOS, A.P. PATSIS
National Hellenic Research Foundation, Athens 116-35, Greece
P.J. BRAY, P.E. STALLWORTH
Department of Physics, Brown University, Providence, RI 02912, USA

The glass formation range in rubidium and caesium borates is greatly enlarged through the use of the alkali oxide instead of the more common alkali carbonate in the batch. Density and glass transition temperature (T_g) measurements were performed on both families of glasses and comparisons to results obtained previously from lithium, sodium, and potassium borate glasses are drawn. ^{11}B NASP NMR data were obtained and compared with Raman spectra in order to model the short-range order found in these glasses. The structures present in these glasses differ considerably from those found in the lighter alkali borate glasses. A discussion of possible structural models is also given.

I Introduction

It has been observed recently that rubidium and caesium borate glasses of very high alkali content can be readily formed from oxide starting materials (1,2,3). This is in contrast to the polycrystalline materials obtained, when the more conventional carbonate starting materials are used. It is the purpose of this paper to report densities and glass transition temperatures along with Raman and NMR measurements for these glasses.

II Experimental Procedure

The glasses were prepared from appropriate quantities of alkali oxide and boron oxide. Composition was controlled using the parameter R, which is defined as the molar ratio of alkali oxide to boron oxide. Batches, 5 to 10 g in mass, were prepared in either platinum, zirconia, or vitreous carbon crucibles. The samples were heated to between 900 and 1000 °C for approximately 15 minutes using an electric muffle furnace. A weight check to verify sample composition was performed after 10 minutes of heating. The resulting melts were formed into glasses via plate quenching or by pouring the melt into a brass mold. Due to the highly hygroscopic nature of these glasses, appropriate measures were taken to ensure that the samples remained dry (3).

The weight check showed a consistent loss of approximately 10-15% of the starting alkali oxide. The observation that small quantities of rubidium are lost was previously made during Raman spectroscopy (4) and density studies (5). The R values assigned to these samples were adjusted to account for this loss. R_{Batch} values reflect the composition of the batch and have not been adjusted for the alkali losses. Samples with R > 1.5 prepared for density measurements were prepared in zirconia or vitreous carbon crucibles only due to the much greater interaction of the samples with platinum crucibles in this range. While samples for T_g determination were prepared in both platinum and vitreous carbon crucibles, it was determined that the difference in results from samples of the same composition prepared in the two types of crucibles was within the experimental error. Raman and NMR samples were prepared in platinum crucibles.

The T_gs were measured using a Perkin-Elmer Model II Differential Scanning Calorimeter (DSC), scanning from 325 to 770 K at a rate of 40 K/min. The sample and reference chambers of the DSC were kept under dry nitrogen. The transition temperature (onset) was determined through the thermal analysis software of Laboratory Microsystems, Troy, NY. Each data point is the average of the individual sample runs made from one batch, with a conservative estimate of the absolute experimental error being ± 5 K.

The densities of these glasses were measured on a Quantachrome model MPY-2

micropycnometer. Mass was measured in a nitrogen atmosphere using a Sartorius model A210P digital balance sensitive to 0.0001 g. A conservative estimate of experimental error in density is ± 0.03 g/cm^3. The densities of low Rb and Cs content borate glasses agreed well with published data (6), after the weight loss of the alkali oxide was accounted for.

Raman measurements were made on a Ramanor HC 2S Jobin-Yvon spectrometer using the 514.5 nm line of a Spectra Physics 165 Argon ion laser and a vacuum cell to avoid hydrolysis and CO_2 uptake. The power level of the laser was approximately 200 mw. A 90° scattering geometry was employed and data were collected at 4 cm^{-1} resolution. Several spectra were acquired at each composition.

Non-adiabatic superfast passage (NASP) techniques were used to acquire the ^{11}B NMR spectra. All measurements were done at 15.70 MHz using a Varian Associates Model V2100B electromagnet, a Varian cross-coil probe, Mid-continent Instruments Model 5005 RF unit, Princeton Applied Research Model HR-8 lock-in amplifier, Matec 110 oscillator, and a Kepco bipolar operational power amplifier (modulation amplifier) and a Nicolet Model 1170 signal averager. All measurements were performed at room temperature. In order to determine the quadrupolar parameters for each spectrum the integrated spectra were computer simulated using a program developed by Taylor and Bray (7).

III Experimental Results and Discussion

The densities of the rubidium and caesium borate glasses are shown in Figure 1 along with the densities of the lighter alkalis previously reported by the Coe College group (8, 9, 10).

A useful method for introducing the alkali dependence of the density is to convert the data to the volume per mole B_2O_3, V_{mol}, determined by (4, 11)

$$V_{mol} = \frac{(R \cdot mw(M_2O) + mw(B_2O_3))}{\rho} \quad (1)$$

where M is the alkali and mw represents molecular weight.
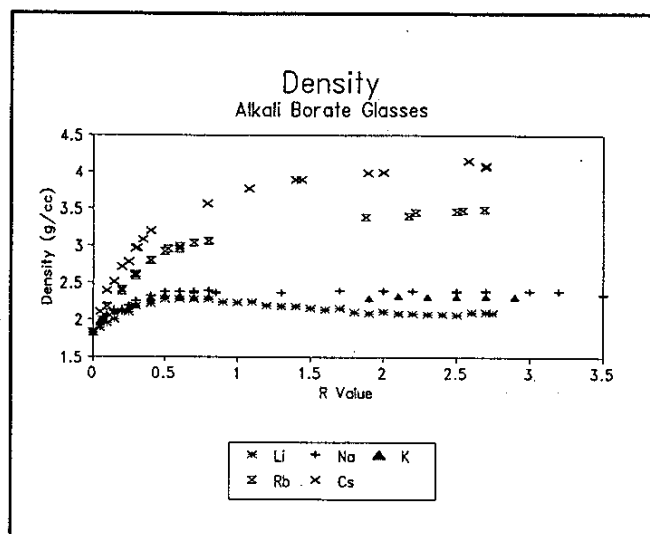
Figure 2 shows V_{mol} versus R for each

Figure 1:
Densities of alkali borate glasses

of the alkali borate glass families. At low R values, the trends are complicated by the formation of four-coordinated borons (f_2 units) from three coordinated borons (f_1 units), and the consequent contraction of the glass network (12,13). The most explicit evidence of this can be found in the lithium borates, where V_{mol} actually decreases until R $\approx$ 0.5.
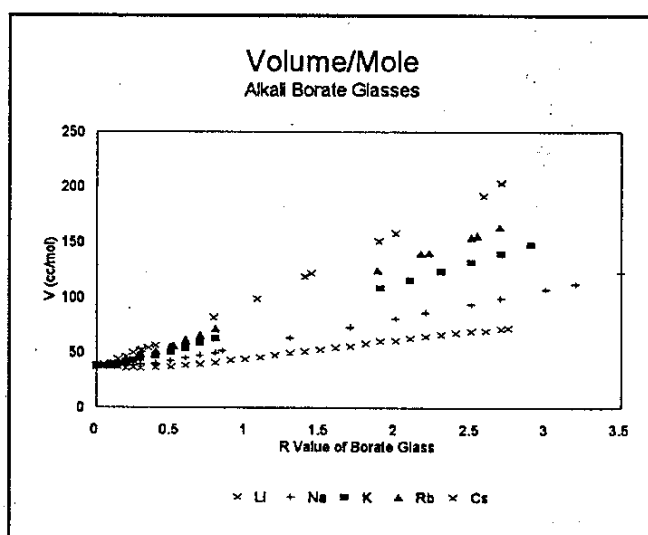

Figure 2:
Volume per mole B_2O_3 in alkali borate glasses

In the other alkali borates the slope of V_{mol} versus R is not as steep in the region $0 \le R \le$

0.5 as it is in the region $0.5 \leq R$.

In the region $0.5 \leq R$, V_{mol} is a linear function of R. This is the result of the dominant formation of nonbridging oxygens (NBOs), a trend consonant with much spectroscopic evidence (13, 14, 15). The slope of this region is dependent on the alkali incorporated with the glass.

A unit change in R in this region results in each boron gaining an alkali ion and half of an oxygen ion. The added volume per boron (ΔV_B) can be expressed as:

$$\Delta V_B = \frac{1}{2} V_{Oxygen} + V_{Alkali} \qquad (2)$$

where V_{Oxygen} and V_{Alkali} are the volumes of the oxygen and alkali ions, respectively. Table 1 lists the ionic radii (adjusted for coordination number) (16, 17, 18, 19, 20), and the resulting volumes for each ion using Equation (2). Table 1 also lists ΔV_B calculated for each of the alkali families using Equation (2).

Table 1

Differential filled space ratios
of alkali borate glasses.

Ion	Radius (Å)	ΔV_B (Å³) Calculated	ΔV_B (Å³) Experimental	Differential Filled Space Ratio
Li	0.78	5.52	13.5	0.41
Na	1.20	10.8	21.7	0.50
K	1.65	22.4	33.7	0.66
Rb	1.77	26.8*	40.9	0.66
Cs	1.95	34.6	52.6	0.66
O	1.19			

ΔV_B was also derived from the slopes of the V_{mol} versus R graph (see Table 1). It is evident that in all cases the calculated ΔV_B is smaller than this experimentally derived ΔV_B. It is proposed that this is because the calculated ΔV_B does not include the empty space that is associated with each borate unit in the actual glass. The ratio of the two sets of ΔV_B, $(\Delta V_B)_{Calculated} / (\Delta V_B)_{Experimental}$, defined as the differential filled space ratio, is also listed in Table 1. It is noted that this ratio increases to a uniform value of 0.66 for the alkali with radii much greater than that of

oxygen, i.e. K, Rb, and Cs. This ratio is close to the maximum value for the filling of space by hard spheres (0.74). This is indicative of the fact that, for glasses incorporating these larger alkalis, in the region $0.5 \leq R$, it is the alkali ions which dominate the filling of space, while the borate units fill voids and charge-compensate the alkali ions. When the smaller alkalis (Li and Na, which have radii less than that of oxygen) are considered, it is evident that the filling of space is controlled by the boron-oxygen network and not the alkali ions. This results in the reduction in the efficiency of filling space to 0.50(Na) and 0.41(Li).

The T_gs of the rubidium and caesium borates, along with those of the lighter alkalis previously reported by the Coe College group (21), are shown as a function of R in Figure 3. It is noted that the data extend over a wide range of alkali concentrations from boron oxide out past the orthoborate composition (R = 0 to R = 4).

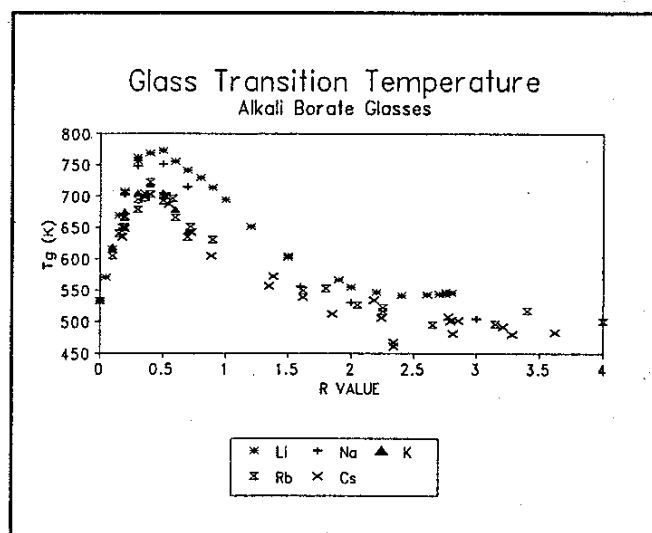The transition temperature rises rapidly initially with increasing R, reaching a

Figure 3:

Glass transition temperatures of alkali borate glasses

maximum at $R \approx 0.4$. As R increases beyond $R \approx 0.4$, there is a wide region of R for which the decrease in T_g is a nearly linear function of R. In the manner of the analyses of Shelby (22), Button *et al.* (23), Martin *et al.* (24), and Affatigato *et al.* (21), it is noted that there is

a strong correlation between the T_g and the fraction of f_2 units present (25). There is a slight discrepancy in the location of the maxima of T_g and f_2, which occurs at $R \approx 0.5$ for the f_2 units (13), as opposed to $R \approx 0.4$ for the T_gs. It is noted that the Tgs correlate better with the average number of bridging boron-oxygen bonds per boron (15). At high R values the T_g levels off, presumably due to the absence of f_2 units. It is noted that for small R the T_gs of Rb and Cs borate glasses are considerably lower than those of the Li and Na borate glasses; at higher R the T_gs of Na, Rb, and Cs borate glasses become comparable while those of Li borate glasses remain higher.
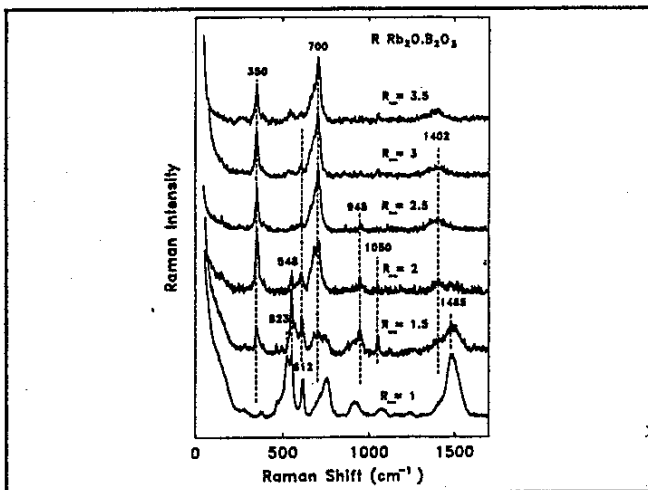

Figure 4(a):
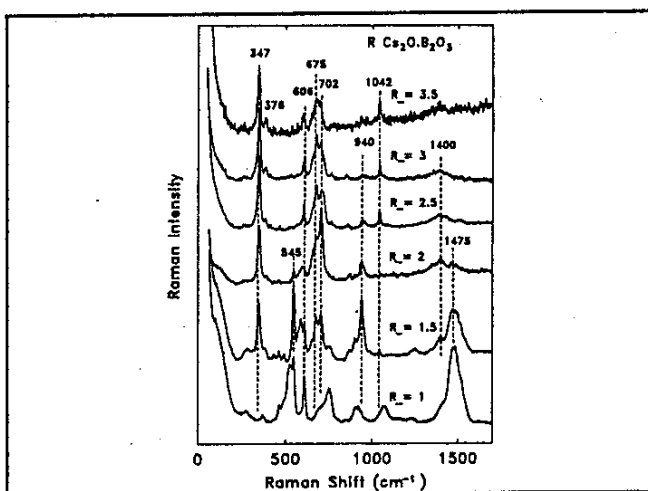**Raman spectra of rubidium borate glasses. Note that R is R_{Batch} in all cases.**

Figure 4(b):
Raman spectra of caesium borate glasses. Note that R is R_{Batch} in all cases.

Figures 4 (a) and (b) present the Raman spectra from the rubidium and caesium borate glasses with $R_{Batch} \geq 1$, respectively. The similarity between the two sets of data are striking and suggestive of a common physical origin for these spectra.

The Raman spectra for the $R_{Batch} = 1$ glasses indicate the presence of ring type metaborate units, f_3, (~610 cm⁻¹, 1400-1600 cm⁻¹) and tetrahedral borate groups (~545 cm⁻¹, 910 cm⁻¹), as well as other units in small amounts (26). The actual positions of these peaks vary a negligible amount between the Rb and Cs cases, with the responses from the Cs glasses being a few cm⁻¹ lower. By R_{Batch} = 1.5 new responses near 675-700 cm⁻¹, 377 cm⁻¹, and 345 cm⁻¹ can be seen. These new frequencies have been hypothesized to result from the formation of a new type of borate arrangement at the orthoborate composition (R = 3), a four-coordinated boron with two NBOs (26). As the alkali concentration increases to near the orthoborate composition (R_{Batch} = 3.5) the spectra for both alkali systems simplifies to just the responses near 345 cm⁻¹, 376 cm⁻¹, 612 cm⁻¹, and 675 cm⁻¹ through 700 cm⁻¹. In addition, the f_3 responses appear as weak features in the spectrum (the weak response near 1050 cm⁻¹ is due to some small amount of CO_2 present in the glasses). It is specifically noted that the responses due to the more usual trigonal pyroborate and orthoborate units (f_4 at ~805 and 1180 cm⁻¹ and f_5 near 860 cm⁻¹)(15, 26) are extremely weak or missing. It is expected that the new tetrahedral orthoborate unit would increase the glass density since, with two bridging oxygens associated with it, it would be more able to form a percolating network, and the tetrahedral nature of the units makes them intrinsically more dense than trigonal units. While it is possible to use this model in the interpretation of the density data, it must be noted that no definitive evidence is provided by the latter for the existence of such a unit.

Figures 5 (a) and (b) present the ¹¹B NASP NMR integrated spectra from the rubidium and caesium borate glasses. Superimposed on these data are the computer simulations of the spectra. Like the Raman spectra shown in Figures 4 (a) and (b), the ¹¹B NASP NMR integrated spectra show a remarkable degree of consistency between the rubidium borate results and those from

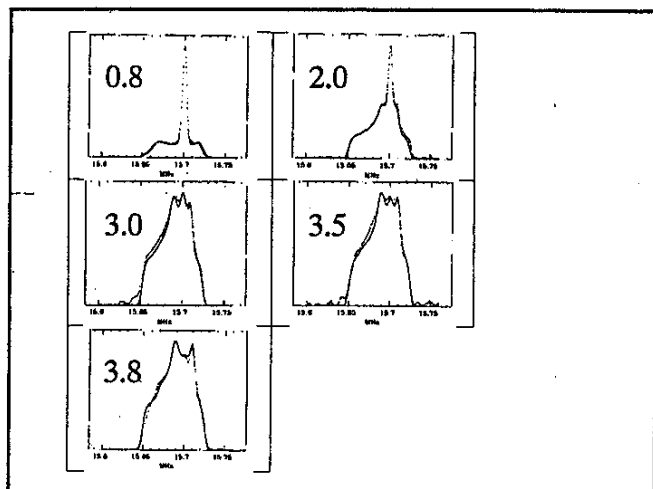caesium borates. In addition, the spectra are fairly static at high values of R.

Figure 5(a):
^{11}B NASP NMR spectra of Rb borate glasses. R_{Batch} values are shown with the spectra.

The spectra from rubidium borate glasses depicted in Figure 5 (a) were deconvoluted into three distinct types of responses (the results for caesium are very similar). These three responses, described in terms of the quadrupole coupling constant and asymmetry parameter, have been previously assigned (27) to symmetric trigonal borons (f_1 and f_5), asymmetric trigonal borons (f_3 and f_4), and tetrahedral borons with all bridging oxygens (f_2). Table 2 lists the fractions of borons in each of these structures.

Table 2

Fractions of the borate units found in high rubidium content borates from ^{11}B NASP NMR

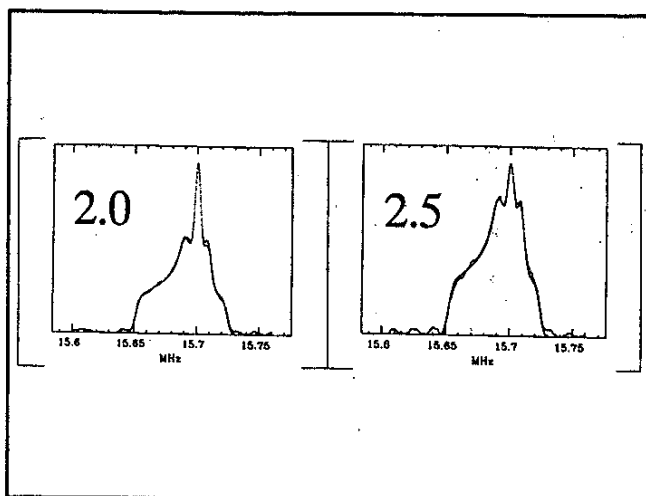| R_{Batch}	f_1 and f_5	f_3 and f_4	f_2
0.8	0.37	0.19	0.44
2.0	0.01	0.86	0.14
3.0	0.01	0.99	0.00
3.5	0.02	0.96	0.02
3.8	0.04	0.95	0.01

Figure 5(b):
^{11}B NASP NMR spectra of Cs borate glasses.
R_{Batch} values are shown with the spectra.

At very high alkali concentrations ($R_{Batch} > 2$) the results obtained show a very large fraction of asymmetric trigonal borate units present in the glass. On the basis of composition these would presumably be in the form of f_4 groups, although the presence of f_3 units can not be ruled out. These results, taken on their own, imply that the glass is undermodified even after taking the loss of alkali in the fusion of the glass into account.

Both Raman and NMR measurements confirm that in the Rb and Cs borate glasses with $R \geq 3$, the presence of trigonal orthoborate units is negligible. Thus, the structure of these glasses differs greatly from that of the analogous Li and Na borates. Both structural techniques indicate that at these high modification levels the structure is dominated by asymmetric borate units (of C_{2v} symmetry), with two non-bridging oxygens per boron. A series of further experiments including NMR, X-ray, crystallization, thermal measurements, and neutron diffraction, are expected to clarify the nature of this unit.

IV. Acknowledgements

References

1. E. I. Kamitsos, G. Chryssikos, A. Patsis, S. A. Feller, K. Farooqui, *Unpublished data.*

2. S. A. Feller, K. Farooqui, P. Pandikuthira, S. Nijhawan, K. Budhwani, Paper 47-G-91F presented at the Electronics, Glass, and Optical Materials Meeting of the American Ceramic Society, Arlington, VA, October, 1991.

3. M. Royle, M. Sharma, S. Feller, J. MacKenzie, S. Nijhawan, Phys. Chem. Glasses 34 (4)(1993) 149

4. S. Koritala, K. Farooqui, M. Affatigato, S. Feller, S. Kambeyanda, S. Ghosh, E. I. Kamitsos, G. D. Chryssikos, A. P. Patsis, J. Non-Cryst. Solids, 134 (1991) 277.

5. E.J. Khaw, Independent study paper, Coe College, 1989

6. O.V. Mazurin, M.V. Streltsina, T.P. Shvaiko-Shvaikovskaya, Handbook of Glass Data, Part B: Single Component and Binary Non-Silicate Oxide Glasses. Elseveir, Amsterdam, 1985.

7. P.C. Taylor and P.J. Bray, J. Mag. Res. 2 (1970) 305

8. M. Shibata, C. Sanchez, H. Patel, S. Feller, J. Stark, G. Sumcad and J. Kasper, J. Non-Cryst Solids 85 (1986) 29

9. A. Karki, S. Feller, H.P. Lim, J. Stark, C. Sanchez and M. Shibata, J. Non-Cryst. Solids 92 (1987) 11

10. H.P. Lim, A. Karki, S. Feller, J. Kasper and G. Sumcad, J. Non-Cryst. Solids 91 (1987) 324

11. K. Takahashi, O. Osaka, R. Furuma, J. Non-Cryst. Solids, 55 (1983) 15

12. P.J. Bray, J.G. O'Keefe, Phys. Chem. Glasses, 4(2)(1963) 37

13. J. Zhong, P.J. Bray, J. Non-Cryst. Solids, 111 (1989) 67

14. E. I. Kamitsos, Ma. Karakassides, G.D. Chryssikos, Phys. Chem. Glasses, 28(5) (1987) 203

15. G.D. Chryssikos, E.I. Kamitsos, M.A. Karakassides, Phys. Chem. Glasses, 31(3) (1990) 109 and 30 (6) (1989) 229.

16. J.E. Huheey, Inorganic chemistry. 1978. Harper, New York

17. F.A. Cotton, G. Wilkinson, Advanced inorganic chemistry. 1988. Wiley & Sons, New York.

18. R. L. Mozzi and B. E. Warren, J. Appl. Crystollogr. 3 (1970) 251.

19. R.D. Shannon, Acta Crystallogr. A, 32 (1976) 751

20. W.H. Zachariasen, Acta Crystallogr. 17(6) (1963) 749

21. M. Affatigato, S. Feller, E.J. Khaw, D. Feil, B. Teoh, O. Mathews, Phys. Chem. Glasses 31 (1) (1990) 19

22. J.E. Shelby, J. Am. Ceram. Soc. 66 (1982) 225

23. D.P. Button, R. Tandon, C. King, M.H. Velez, H.L. Tuller, D.R. Uhlmann, J. Non-Cryst. Solids 49 (1982) 129

24. S.W. Martin, C.A. Angell, J. Non-Cryst. Solids 66 (1984) 429

25. B.C.L. Chong, S.H. Choo, S. Feller, B. Teoh, O. Mathews, E.J. Khaw, D. Feil, K.H. Chong, M. Affatigato, D. Bain, K. Hazen, K. Farooqui, J. Non-Cryst. Solids 109 (1989) 105

26. G. D. Chryssikos, E. I. Kamitsos, A. P. Patsis, M. A. Karakassides, Matr. Sci. Eng. B7 (1990) 1.

27. Y. H. Yun and P. J. Bray, J. Non-Cryst. Solids 27 (1978) 363.